Proceedings of the Institute of Acoustics

THE MODELLING AND DESIGN OF CONTROLLABLE COMPOSITE TRANSDUCERS.

R. Hamilton and G. Hayward

Ultrasonics Research Group, Department of Electronic and Electrical Engineering, The University of Strathclyde, 204 George Street, Glasgow, G1 1XW, Scotland.

ABSTRACT

Some performance characteristics of controllable composite transducers, comprising an apodised disc piezoceramic transmitter and an integral polymer film receiver are described and verified on an experimental basis. Apodisation of the transmitter, via a resistive taper electrode design is utilised to control the spatial distribution of the generated ultrasonic field. The wideband receiver may comprise a single element polyvinylidene (PVDF) layer or alternatively can be configured as a one dimensional multi-element annular array. Using this combination the composite devices are shown to produce enhanced signal quality, particularly in applications such as imaging and materials characterisation where some form of inverse signal processing is required.

1. INTRODUCTION

Conventional thickness mode piezoelectric transducers often suffer physical limitations which can restrict severely their application range. Examples include aperture diffraction and multi-mode mechanical vibration, both of which introduce complex field behaviour with a resultant spatial variation in acoustic pulse profile. Data interpretation with respect to propagation medium characteristics and any associated inverse signal processing is thus limited to restricted regions within the transducer sound field.

This problem has attracted considerable attention and several techniques for controlling the spatial field of disc transducers have been reported in the literature [1,2,3]. One method which the authors have found successful [3] is illustrated in Figure 1, where a continuously varying resistive taper and appropriate choice of electrode pattern permit suppression of plane or edge components associated with circular aperture diffraction. As shown in Figure 1, with 'edge wave' suppression, the resistive taper is utilised in order that the applied electric field decreases from a maximum at the centre to zero at the edge in a controlled fashion. A particular feature of such a shaded transmitter is that the radial modes associated with some ceramic devices are suppressed [3]. Alternatively, the resistive taper is employed such that with 'plane wave' suppression the electric field is maximum at the disc edge and is reduced to zero in the centre, again in a controlled manner. Apodisation in this fashion results in axial focusing which is particularly applicable to imaging applications [3].

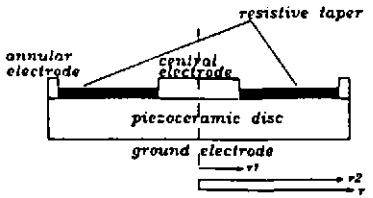

Figure 1: Apodisation of transmitter aperture.

The Modelling and Design of Controllable Composite Transducers.

Although attractive, such apodised structures, with their fixed beam characteristics, possess limited flexibility. This problem may be overcome by incorporation of a separate PVDF receiver positioned within the front face matching layer. When configured as an annular array, this device provides wideband reception in conjunction with variable beamforming for specific applications.

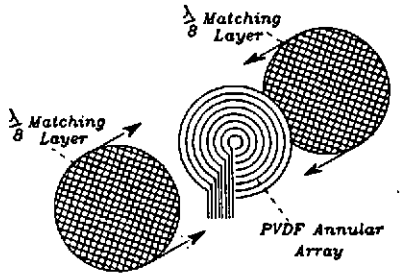

Figure 2: Typical receiver configuration within composite structure.

The combination of an apodised ceramic transmitter (which may be utilised for reception) and PVDF reception array is particularly attractive for operation into low impedance media, where the relative sensitivities of the two transducer materials are employed for maximum benefit. A typical receiver configuration is shown in Figure 2, where each element may be configured as a separate receiver or electronically controlled to enable reception beamforming.

In the following sections the principal features of the apodised transmitters are reviewed, followed by a series of examples illustrating the enhanced behaviour of the new composite devices.

2. REVIEW OF TRANSMITTER CHARACTERISTICS

The theory covering behaviour of the apodised transmitters is described elsewhere [3] and only the main results are repeated here. In a centre shaded device (CSD) the excitation voltage distribution across the aperture of a disc transducer is shown in Figure 3a and described by Equation 1.

$$V(r) = \frac{V_s \ln\frac{r2}{r}}{\ln\frac{r2}{r1}} \qquad r1 \le r \le r2 \qquad \text{Equ. 1}$$

Where Vs is the applied excitation voltage. This type of transducer is expected to demonstrate smooth field characteristics, with minimum spatial variance of the radiated pressure wavelet[3].

The Modelling and Design of Controllable Composite Transducers.

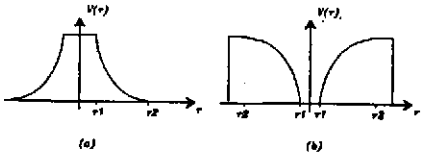

Figure 3: The voltage distribution aperture functions of (a) a centre shaded device (CSD) (b) an edge shaded device (ESD).

On the other hand, with an edge shaded device (ESD), the aperture distribution decays from the transducer periphery towards the centre in a controlled manner. The appropriate voltage distribution function is shown in Figure 3b and described by Equation 2.

$$V(r) = \frac{V_s \ln \frac{r}{r1}}{\ln \frac{r2}{r1}} \qquad r1 \le r \le r2 \qquad \text{Eqn. 2}$$

This type of device, although displaying near field structural variation, is expected to generate a highly focused beam which is collimated along the transducer axis [3].

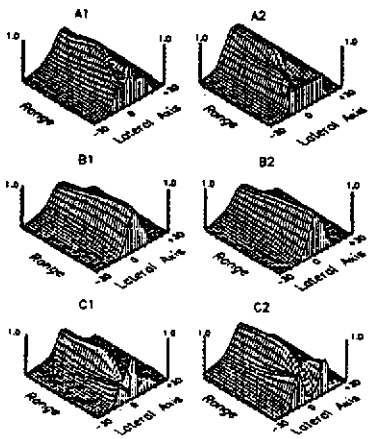

Figure 4: Field directivity of (A) Conventional disc transmitter (B) Centre shaded device (C) Edge shaded device. 1-Experiment 2-Theory

The principal features of both CS and ES transducers are illustrated in Figure 4 which compares the field directivity characteristics with those of non-apodised 'conventional' transducers. In each case the transducers comprised 30mm diameter PZT-5A discs operating under transient conditions at a centre frequency of 1MHz into a water load. A scanning wideband membrane hydrophone was used to detect the peak pressure component which is plotted as a function of axial and lateral distance.

It is apparent that the CS transmitter generates a relatively smooth field structure when compared with the other devices, while the ES device demonstrates improved axial focusing beyond the near/far field boundary. Theoretical predictions are in broad agreement except in the very near field where radial and head wave interference may be obseved on the experimental data. It is interesting to quantify the extent of spatial invariance associated with the new transducer structures. Table 1 indicates the normalised cross-correlation coefficient obtained for the three transducers at axial ranges of 20mm, 60mm, and 120mm.

Table 1:Correlation table of transmitted experimental axial profiles.

range	Unshaded transmitter	Centre shaded transmitter	Edge shaded transmitter
20mm	1.000	1.000	-
40mm	0.449	0.991	1.000
120mm	0.645	0.961	0.840

Note that no measurement was performed for the ESD at 20mm owing to the strong radial mode activity present in this region. In each case, the wavelet at an axial range of 20mm (40mm ESD) was correlated against that measured at other axial positions. It is apparent that the CSD demonstrates little spatial variance at all ranges, while the ESD is reasonably consistent in the far field.

The apodised structures also possess an additional important feature. Owing to the clamping effect of the resistive taper, the upper spectral harmonics are emphasised with respect to the fundamental frequency. This is illustrated by comparing the impedance magnitude spectra shown in Figure 5. The relatively wideband behaviour of the shaded devices is readily apparent.

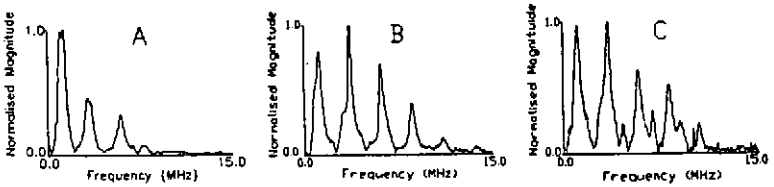

Figure 5: Impedance magnitude spectra of (A) Conventional disc transmitter (B) Centre shaded device (C) Edge shaded device

3.POTENTIAL APPLICATIONS FOR THE NEW TRANSDUCERS

3.1 Control of Wavelet Profile (pre-filtering)

Generation of a pre-determined acoustic waveshape is often required for high resolution imaging and material characterisation [4]. Consider the following frequency domain expression describing transducer output.

The Modelling and Design of Controllable Composite Transducers.

$$Y(f) = X(f) \times E(f) \qquad \text{Eqn. 3}$$

where Y(f) represents the response of the transducer.
X(f) describes the transducer transfer function.
E(f) represents the voltage excitation function applied to the transducer.

The excitation function required to generate a specific transducer output may be evaluated from inversion of X(f) in Equation 3. That is

$$|E(f)|\exp(j\phi_E) = \frac{|Y(f)|\exp(j\phi_Y)}{|X(f)|\exp(j\phi_X)} \qquad \text{Eqn. 4}$$

As X(f) tends to zero then the corresponding component in E(f) tends to infinity. In order to protect against such discontinuities in the resulting spectrum, the spectral components are redefined by setting a threshold as described by Equation 5.

$$\begin{matrix} |X(f)| = |X(f)| & |X(f)| \geq c \\ |X(f)| = c & |X(f)| < c \end{matrix} \qquad \text{Eqn. 5}$$

An appropriate threshold was set by placing the threshold at 50dB below the peak of the magnitude spectrum. The thresholding operation does not influence phase information and the phase associated with each spectral component is retained in the modified spectrum. The required excitation function is obtained by Inverse Fourier Transformation after spectral division with the modified spectrum.

Representative results for the three transducers are shown in Figure 6, where attempts have been made to generate a bipolar square wave in a water tank. It is apparent that improved performance is obtained for the apodised structures, as a direct consequence of the extended operational bandwidth.

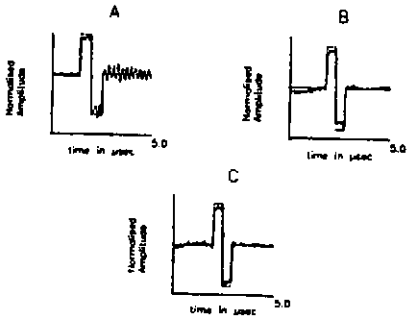

Figure 6: Prefiltering to a bipolar square wave of (A) Conventional disc transmitter (B) Centre shaded transmitter (C) Edge shaded transmitter.

The Modelling and Design of Controllable Composite Transducers.

3.2 Resolution Enhancement (Post-Filtering).

It is also possible to improve the resolution of a target structure by means of suitable deconvolution or post-filtering. Unfortunately optimal performance is rarely achieved owing to the non-minimum phase characteristics and spatial variance associated with conventional ultrasonic data [5]. The improvement offered by the new transducers is illustrated in Figure 7, indicating the reconstructed acoustic impulse response of a layered target using a Two-Sided Weiner Filter [6]. A target thickness of 50mm (crown glass block in water) was selected to emphasise the influence of spatial variation in the received pulse profiles. It is apparent that even with this relatively crude time domain filter, improved performance has been achieved from the apodised transmitters.

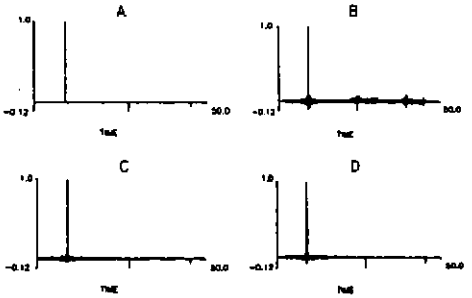

Figure 7: Acoustic impulse response of a 50mm glass block in water. (A) simulated acoustic impulse response (B) deconvolved impulse response of conventional disc transducer (C) deconvolved impulse response of centre shaded transmitter with 30mm diameter PVDF receiver (D) deconvolved impulse response of edge shaded transmitter with 6mm diameter PVDF receiver.

3.3 Imaging Performance.

As a direct result of the finite apeture, imaging within the very near field of conventional transducers produces object smearing. The improvement offered by a broad beam centre shaded device incorporating an 8-element, half-wavelength annular array is illustrated in Figure 8. Here, reception delay beamforming [7] was utilised to maximise the receive response and focus the annular array.

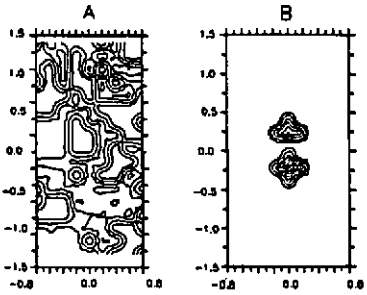

Figure 8: Imaging results obtained (A) from a 30mm diameter conventional disc transducer with 50% thresholding on received data (B) from a centre shaded transmitter incorporating a PVDF annular array receiver with 50% thresholding on received data.

The objects, which were subject to a raster scan (2mm horizontal and 2mm vertical) in a water tank, comprised a pair of 2mm diameter circular steel targets separated by a distance of 6mm and positioned 10mm from the transducer surface. Resultant C-scan images are shown in Figure 8 A-B, for a conventional transducer (A) and the CSD-array combination (B). In each case the transducer diameter was 30mm, with a centre frequency of 1MHz. The improvement obtained from the composite structure is obvious.

4. CONCLUDING REMARKS

A range of ceramic-PVDF transducers have been described and a selection of results indicating their potential for imaging and structural characterisation have been described. Although more complex from a constructional viewpoint, it is anticipated that the new devices will lead to improved inverse signal processing in ultrasonic applications. Indeed the combination of an efficient, apodised piezoceramic device and an integral piezo-polymer film (both of which may be utilised in transmission or reception), greatly enhances transduction and application flexibility. Evaluation of the new devices for pre/post filtering, layer peeling and improved imaging is currently underway at Strathclyde and will be reported at a later date.

5. REFERENCES

[1] J.P. Weight 'New Transducers for High Resolution Ultrasonic Testing', NDT International, Vol 17, No 1, Feb 1984, pp3-8

[2] R.O. Claus P.S. Zerwekh ' Ultrasonic Transducer with a Two-Dimensional Gaussian Field Profile', IEEE Trans. on Sonics and Ultrasonics, Vol30, No 1, Jan 1983, pp36-39.

[3] G. Hayward, R. Hamilton, B. Kanani, and D.A. Reilly 'A Thin Film Technique for Spatial Apodisation of Disc Piezoelectric Transducers', Accepted for publication J. Acoust. Soc. Am.

[4] J. Schmolk et al 'Generation of Optimal Input Signals for Ultrasonic Pulse Echo Systems', IEEE Ultrasonics Symposium, 1982, pp 929-934

[5] G. Hayward, J.E. Lewis 'Comparison of Some Non-Adaptive Deconvolution Techniques for Resolution Enhancement of Ultrasonic Data', Ultrasonics, 27, 1989, pp155-163.

[6] A.J. Berkout 'Least-Squares Inverse Filtering and Wavelet Deconvolution', Geophys, Vol 42, No 7, Dec 1977, pp1369-1383

[7] P.D. Corl, P.M. Grant, G.S. Kino 'A Digital Synthetic Focus Acoustic Imaging System for NDE', IEEE Utrasonics Symposium, 1978, pp263-268.